

# Flow Enhancement of Shear-Thinning Liquids in Capillaries Subjected to Longitudinal Vibrations

Jürg Ellenberger and Rajamani Krishna\*

DOI: 10.1002/cite.201700028

*Dedicated to Prof. Dr. Frerich J. Keil on the occasion of his 70th birthday*

Application of sinusoidal vibrations in the longitudinal direction causes a significant enhancement in the flow rate of shear-thinning carboxymethylcellulose and polyacrylamide solutions inside capillaries. Depending on the vibration frequency and amplitude, flow enhancements of up to a factor of 9.6 have been realized. Video imaging of a tracer particle inside the tube provides insights into the liquid motion. In particular, it should be noted that the phase shift between the sinusoidal motion of the tube wall and the liquid inside the tube is of high importance in determining the flow enhancement factor.

**Keywords:** Carboxymethylcellulose, Flow enhancement, Polyacrylamide, Polymer solutions, Shear-thinning liquids, Sinusoidal vibrations

*Received:* April 24, 2017; *revised:* August 06, 2017; *accepted:* August 07, 2017

## 1 Introduction

Since the early work of Barnes et al. [1], several other investigations [2–19] have demonstrated that the imposition of pulsations, oscillations, vibrations, or shaking on the flow of a shear-thinning non-Newtonian liquid in tubes or capillaries has the effect of enhancing the flow rate above the steady-state value, i.e., the value obtained under conditions without periodic disturbances to the flow. In practice, such flow enhancements are of interest in polymer extrusion, molding, and spinning [10, 12]. Other potential applications include the reduction in the resistance to the flow of blood [15] and of chocolate [16]. Vibrations and oscillations can also enhance gas-liquid contacting [20].

Deshpande and Barigou [18] investigated the flow enhancement of a carboxymethylcellulose (CMC) solution in a 4-mm capillary tube that was subjected to sinusoidal vibrations in the longitudinal (axial) direction. In the experimental work reported here, that follows up on the work of Deshpande and Barigou [18], flow enhancement was investigated in two types of shear-thinning liquids, namely, CMC solution and polyacrylamide (PAA) solution that also has a viscoelastic character. The influence of a wide range of parameters was investigated, including vibration frequency  $f$ , vibration amplitude  $\lambda$ , capillary diameter  $D$ , and pressure gradient  $\Delta P/L$ . In some cases, the published CFD simulation results [18] are compared with the experimental results of the present work. Insights into flow enhancement are gained by also experimentally tracking the sinusoidal motion of the tube wall and of the liquid inside the tube by means of high-speed video imaging of tracer particles.

## 2 Experimental Setup and Systems Studied

The polymer solutions flow from a 1-L glass vessel under constant external pressure into a capillary tube with a length  $L$  of 0.500 m. The experiments are carried out in glass capillaries of three different (nominal) diameters of 1 mm (i.d. = 1.155 mm), 2 mm (i.d. = 2.156 mm), and 4 mm (i.d. = 3.961 mm). The connection between the glass vessel and the capillary is a flexible silicone tube of 8 mm inner diameter and a length of 0.25 m. The diameter of this silicone tube is much larger than the diameter of the capillaries used in this study in order to minimize the pressure loss and flow disturbance between the vessel and the capillary. The glass capillaries were vertically mounted onto a shaft of an air-cooled vibration exciter (TIRAvib 5220, TIRA Maschinenbau GmbH, Germany). In this way, vertical displacements of the shaft at specific amplitudes  $\lambda$  and frequencies  $f$  fully corresponded to vibrations of the capillary. The vibration exciter was coupled to a power amplifier and controlled from a personal computer using SignalCalc 550 vibration controller software (Data Physics Corporation, USA).

A schematic picture of the experimental setup, which is essentially similar to that described by Deshpande and Barigou [18], is shown in Fig. 1. The applied frequencies ranged

---

Dr. Jürg Ellenberger and Prof. Dr. Rajamani Krishna  
r.krishna@contact.uva.nl  
University of Amsterdam, Van't Hoff Institute for Molecular Sciences, Science Park 904, 1098 XH Amsterdam, The Netherlands.

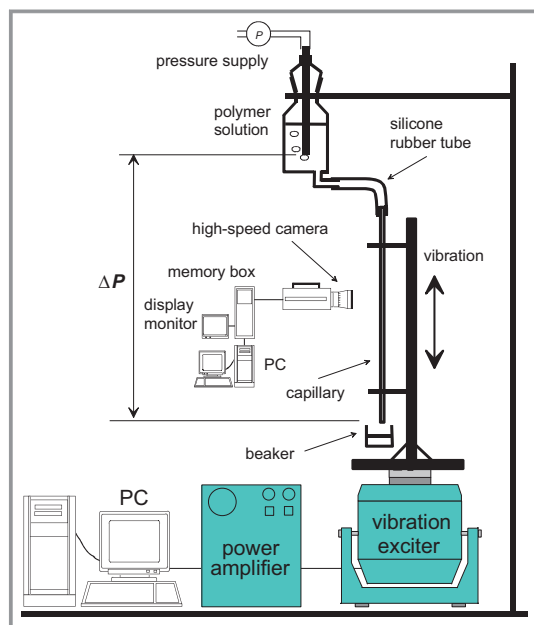


**Figure 1.** Experimental setup for the investigation of the influence of low-frequency vibrations on the flow through capillaries.

from 5 to 40 Hz and the amplitudes from 1.5 to 10 mm. The dimensionless vibration intensity  $\Gamma = \lambda(2\pi f)^2/g$  was varied from 0.5 to 14. In this paper, the amplitude of vibration is defined as the absolute value of the maximum positive or negative displacement of the vibration exciter from its rest position. The vibration exciter was programmed to generate sinusoidal oscillations.

The mass flow rate was determined by measuring the weight of liquid at the exit of the capillary during a predetermined time interval. The pressure drop  $\Delta P$  varied from 5.6 to 16 kPa. To track the flow characteristics, i.e., the center-line velocity and amplitude, of the fluids flowing within the capillary tube, coal tracer particles with a density of  $500 \text{ g L}^{-1}$  and a size in the range of  $0.4 \text{ mm} < d_p < 0.72 \text{ mm}$  were injected into the capillary. The coal particles are suspended in the glycerol solution. High-speed video movies of the coal particle flowing within the capillary were recorded. A Photron FASTCAM Ultima 40K high-speed video camera was used, which has the capability of recording at between 30 frames per second (fps) and 40 500 fps. The camera was connected to a memory box, which allowed instantaneous storing of the movies, as well as a display monitor, which enabled real-time viewing of the movies. Lighting for the movies was provided by a single Dedotec dedocool 250 W halogen photo-optic lamp. This lamp enabled sufficient illumination without increasing the ambient temperature.

After each video recording, the obtained data were transferred from the memory box to a personal computer for analysis. By frame-by-frame analysis of the video recordings, the velocity and amplitude of tracer particles could be determined. These values are representative of the flow con-

ditions at the center line of the capillary. Sample video recordings are available for online viewing [21].

Experiments were carried out with aqueous solutions of two different polymers: (1) 0.7 wt % high viscosity-grade CMC sodium salt with a typical molecular weight of  $7 \cdot 10^5 \text{ g mol}^{-1}$  (Sigma-Aldrich, USA) and a density of  $1002 \text{ kg m}^{-3}$ , and (2) 0.5 wt % PAA with a typical molecular weight of  $1 \cdot 10^6 - 3 \cdot 10^6 \text{ g mol}^{-1}$  (Separan AP-30, Dow Chemicals, USA) and a density of  $1001 \text{ kg m}^{-3}$ . Additionally, experiments were also carried out with an aqueous solution of 90 wt % glycerol having Newtonian character with a dynamic viscosity  $\eta$  of  $0.184 \text{ Pa s}$  and a density of  $1235 \text{ kg m}^{-3}$ . All the experiments reported in this paper were conducted in the laminar flow regime, and the highest Reynolds number  $Re$  obtained was 21, for PAA solution in the 4 mm capillary at a flow enhancement factor of 2.3.

The apparent viscosity  $\eta_a$  as function of the shear rate  $\dot{\gamma} (= 8\langle u \rangle/D)$  of the two polymer solutions shown in Fig. 2 has been calculated from the measured pressure drop  $\Delta P$  and mass flow  $\phi_m$ :

$$\eta_a = \frac{\tau}{\dot{\gamma}} = \frac{\Delta P D / (4L)}{8 \langle u \rangle / D} = \frac{\Delta P D^4 \rho \pi}{128 L \phi_m} \quad (1)$$

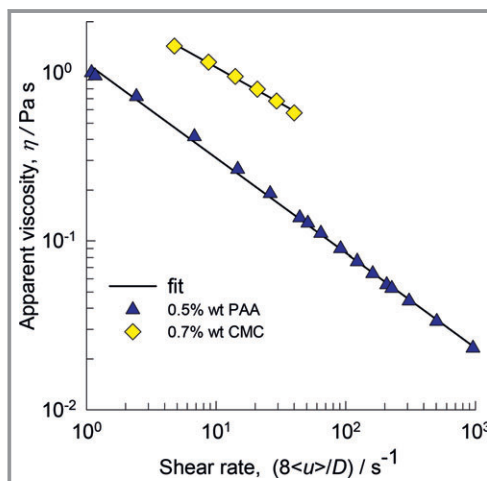


**Figure 2.** Power-law fits for the apparent viscosity of the CMC and PAA solutions used in this work.

Eq. (1) is only valid for Newtonian liquids, but it gives also a good approximation for shear-thinning liquids. The apparent viscosity can be described by the power-law model

$$\eta_a = k \dot{\gamma}^{n-1} \quad (2)$$

with  $k = 2.87$  and  $n = 0.571$  for 0.7 wt % CMC and  $k = 1.13$  and  $n = 0.437$  for 0.5 wt % PAA. It should be noted that PAA additionally has viscoelastic properties [22].

### 3 Experimental Results Obtained with Glycerol Solutions

First, it is established that there is no flow enhancement for the flow of a Newtonian fluid through a capillary. The experimental results with 90 wt % aqueous solution of glycerol in a 2-mm capillary are summarized in Tab. 1. The data in Tab. 1 clearly show that a Newtonian liquid does not exhibit any flow enhancement under vibration conditions and the flow enhancement factor  $\phi_v/\phi_{v,0}$ , i.e., the flow rate under vibration conditions  $\phi_v$  divided by the flow rate at steady-state non-vibration condition  $\phi_{v,0}$  remains at a constant value around unity.

**Table 1.** Experiments with 90 wt % glycerol solution in 2-mm capillary. The pressure drop in all experiments was maintained at  $\Delta P = 7.8$  kPa.

Experiment	$\lambda$ [mm]	$f$ [Hz]	$\phi_v$ [ $10^{-8} \text{ m}^3 \text{ s}^{-1}$ ]	$\langle u \rangle$ [ $\text{m s}^{-1}$ ]
1	0	0	4.49	0.0123
2	2.5	15	4.42	0.0121
3	5	5	4.42	0.0121
4	5	10	4.43	0.0121
5	5	15	4.63	0.0127
6	7.5	15	4.48	0.0123
7	10	5	4.42	0.0121
8	10	10	4.48	0.0123

Fig. 3 shows the analysis of a high-speed video movie of the glycerol solution (experiment 5 in Tab. 1) at  $f = 15$  Hz and  $\lambda = 5.0$  mm. The symbols represent data that have been obtained from frame-by-frame analysis of the movie. The sinusoidal motion of the capillary tube is described by

$$y = \lambda \sin(2\pi ft + \delta_c) \quad (3)$$

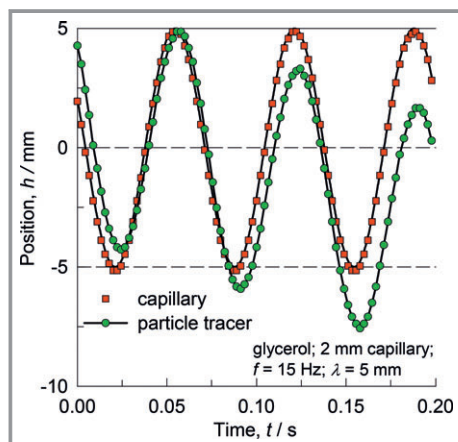


**Figure 3.** Sinusoidal wave motion of the capillary and motion of a tracer particle for the flow of the glycerol solution through the 2-mm capillary.  $f = 15$  Hz,  $\lambda = 5.0$  mm.

with  $\delta_c$  as the phase shift of the capillary. The movement of the tracer particle flowing through the center line of the capillary can be described by

$$y = a \sin(2\pi ft + \delta_p) - b - ut \quad (4)$$

where  $a$  is the amplitude of the tracer particle,  $b$  is the vertical shift parameter, which shifts the curve to the right vertical position,  $\delta_p$  is the phase shift of the particle, and  $u$  represents the downwards velocity of the particle, corresponding to the center-line velocity of the liquid inside the tube. For experiment 5 shown in Fig. 3, this procedure resulted in a value of  $a = 4.98$  mm, a small phase shift  $\delta = \delta_c - \delta_p = 0.24$  and a particle tracer velocity  $u = 0.024 \text{ m s}^{-1}$ . It should be noted that the amplitude of the particle is very close to the amplitude of the capillary and the center-line velocity  $u$  of the particle is twice the average liquid velocity  $\langle u \rangle$  (Tab. 1) corresponding to the laminar velocity profile of a Newtonian liquid.

### 4 Experimental Results Obtained with CMC Solution

For a shear-thinning liquid such as CMC, the application of vibrations will reduce the apparent viscosity and result in increased flow. Fig. 4 shows the experimental data for the flow enhancement factor for the 0.7 wt % CMC solution as a function of the vibration frequency in capillaries of 2 mm (Fig. 4a), and 4 mm (Fig. 4b) diameter. For a given vibration amplitude, the enhancement factor increases with the vibration frequency and vice versa. These results are consonant with the experiments of Deshpande and Barigou [18] and also with their CFD simulations.

Increasing the steady-state flow rate in a capillary by increasing the pressure gradient  $\Delta P/L$  results in a lower flow enhancement factor at constant vibration conditions, because the vibrational contribution becomes relatively smaller. Fig. 5 shows that increasing  $\Delta P/L$  leads to a decrease in the flow enhancement factor for the CMC solution flow in 2-mm and 4-mm capillaries with  $f = 20$  Hz. These results are in agreement with the CFD simulations of Deshpande and Barigou [18]; however, they did not perform experiments to confirm this trend.

Fig. 6 shows two examples of the high-speed movie analysis of the sinusoidal motion of the capillary tube and the tracer particle for 0.7 wt % CMC in a 4-mm capillary at vibration frequencies of 20 Hz (Fig. 6a) and 35 Hz (Fig. 6b). When compared to the corresponding sinusoidal motion for a Newtonian liquid (cf. Fig. 3), the first point to note is that there is a larger phase shift between the sinusoidal motion of the capillary tube and that of the tracer particle within the tube. This shift,  $\delta$ , quantified by  $\delta_c - \delta_p$ , appears to increase with increasing vibration frequency (Fig. 7a). It counteracts the sinusoidal movement of the capillary resulting in a lower flow enhancement factor than expected without phase shift. Fig. 7a shows that the phase shift in the 4-mm capillary is much larger compared to the phase shift in the 2-mm capillary. This explains

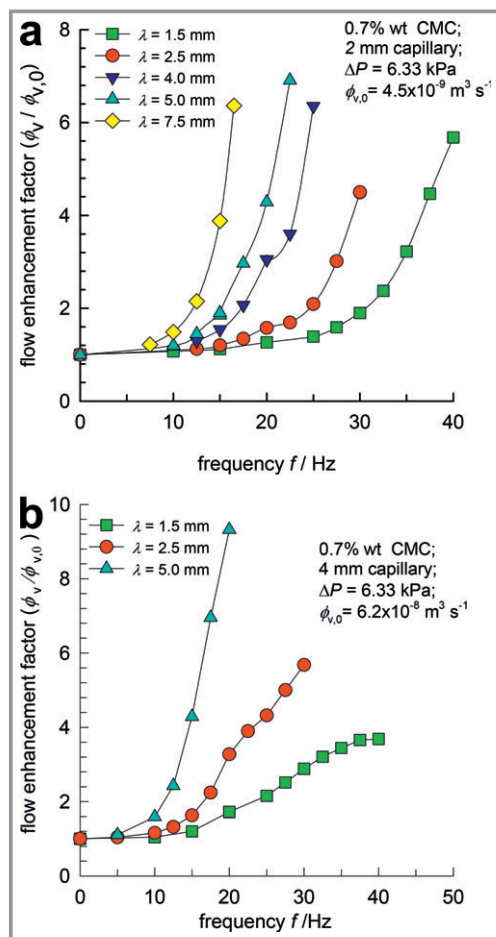


**Figure 4.** Flow enhancement factor of a 0.7 wt % CMC solution as function of the vibration frequency in capillaries of a) 2 mm, and b) 4 mm diameter.

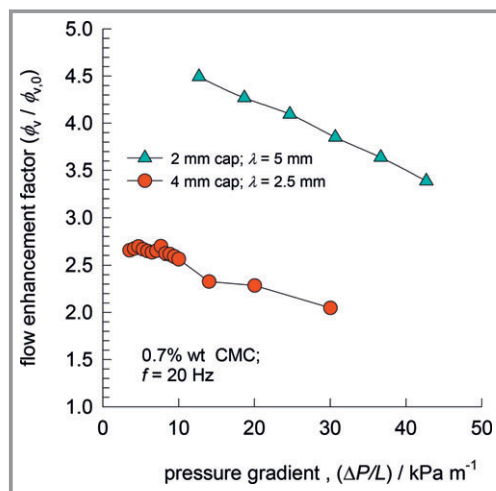


**Figure 5.** Influence of the pressure gradient on the flow enhancement factor for a 0.7 wt % CMC solution in 2-mm and 4-mm capillaries with  $f = 20$  Hz.

why the enhancement factor in the 4-mm capillary shows the tendency to reach a plateau value (cf. Fig. 4b).

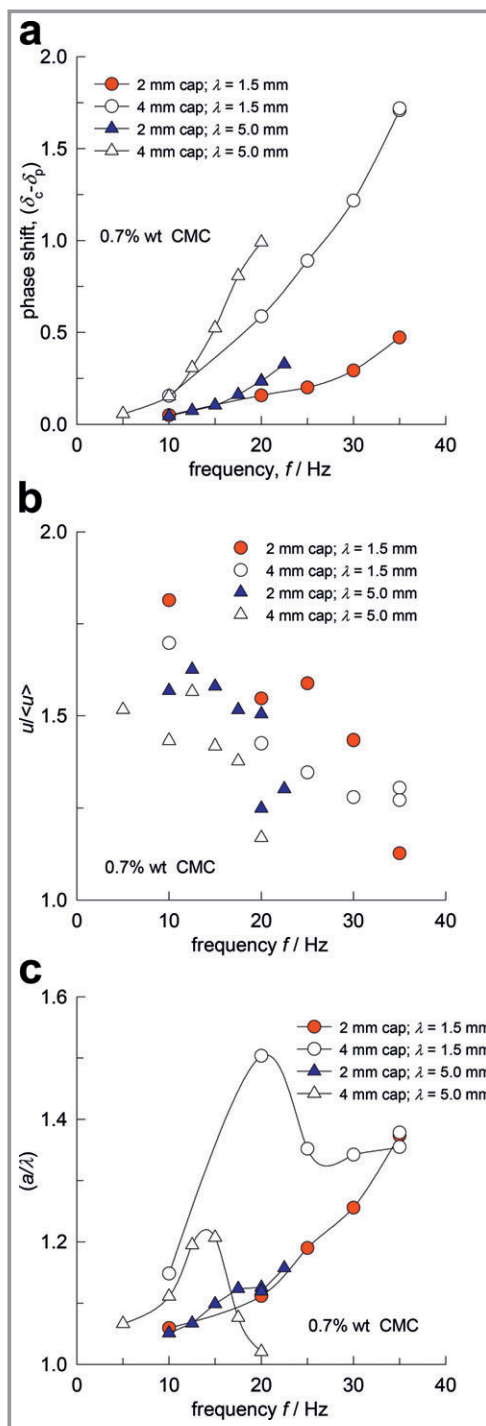


**Figure 6.** Typical examples of the high-speed movie analysis of the sinusoidal motion of the capillary tube and the tracer particle for 0.7 wt % CMC in a 4-mm capillary at vibration frequencies of a) 20 Hz and b) 35 Hz.

The center-line liquid velocity (as represented by tracking the tracer particle) is significantly lower than the value of 2, typical for Newtonian liquids (Fig. 7b). The amplitude of the sinusoidal motion of the tracer particle ( $a$ ) is also significantly higher than that of the capillary tube ( $\lambda$ ) (Fig. 7c). It

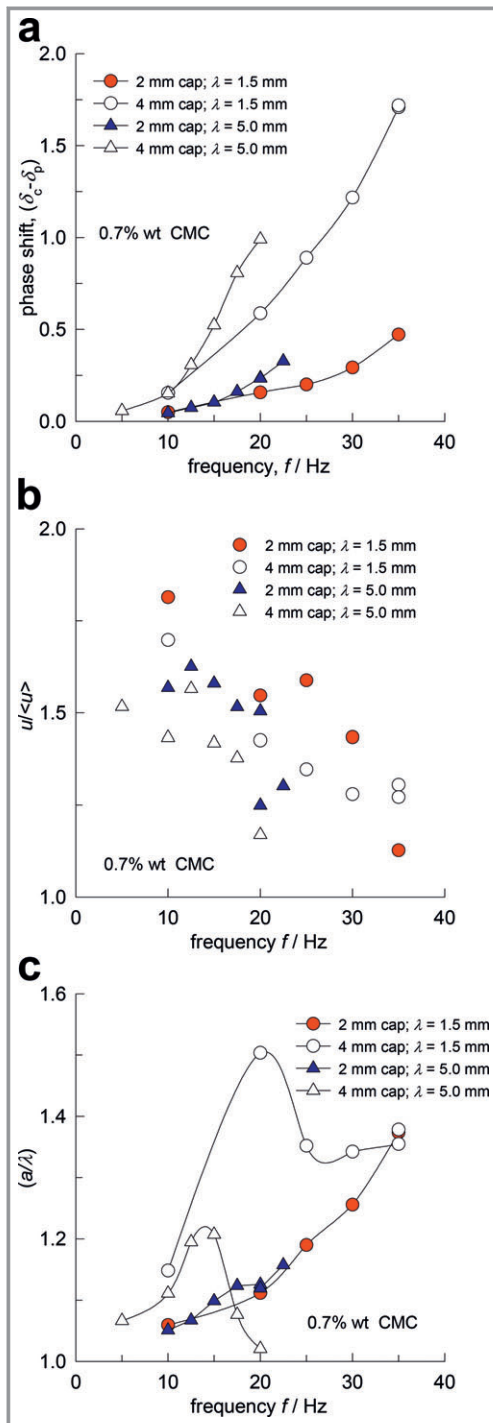


**Figure 7.** Quantitative analysis of the sinusoidal trajectories followed by the capillary tube and the tracer particle for the flow of 0.7 wt % CMC in capillaries of 2 and 4 mm diameter. a) Phase shift  $\delta_c - \delta_p$ , b)  $u/\langle u \rangle$ , and c)  $a/\lambda$  of a tracer particle flowing in the center line of the capillary during vibration.

can be seen that  $a/\lambda$  vs  $f$  exhibits a maximum for the 4-mm capillary tube.

For different vibration frequencies and adjusting the amplitude in such a way that the vibration intensity

$\Gamma = \lambda(2\pi f)^2/g$  remains constant, Deshpande and Barigou [18] found, by CFD simulations, an almost constant value of the flow enhancement factor, which is in qualitative agreement with the experiments in the 2-mm capillary conducted in this study (Fig. 8a). However, as it can be seen in Fig. 8b, this relation does not apply to the data of the 4-mm capillary. It is concluded that the vibration intensity  $\Gamma$  does not uniquely determine flow enhancement.

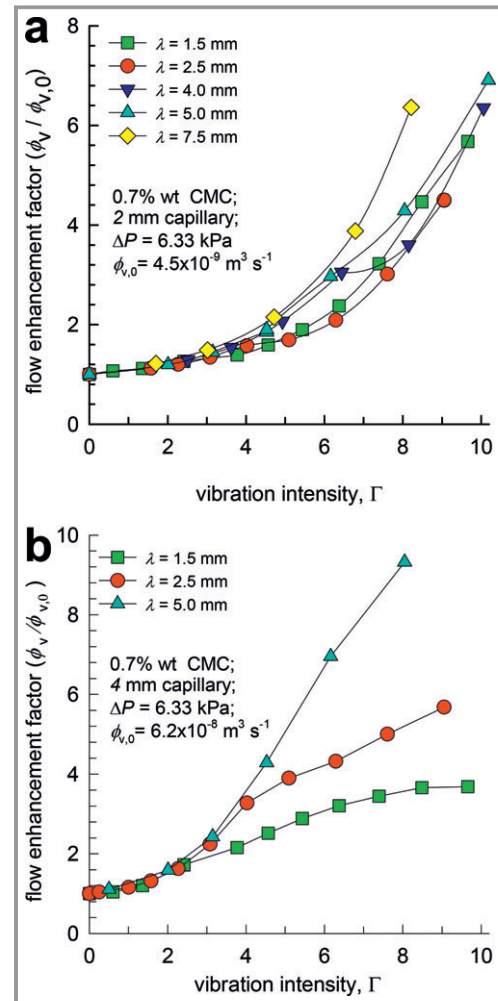


**Figure 8.** Flow enhancement factor of a 0.7 wt % CMC solution as function of the vibration intensity in capillaries of a) 2 mm, and b) 4 mm diameter.

## 5 Experimental Results Obtained with PAA Solution

Fig. 9 shows the sinusoidal trajectories of the tube and the tracer particle for 0.5 wt % PAA in the 2-mm capillary at vibration frequencies of 10 Hz (Fig. 9a) and 20 Hz (Fig. 9b). With increased vibration frequency, the increase in the phase shift is considerably more significant than for CMC (cf. Fig. 6). Fig. 10 compares the phase shift  $(\delta_c - \delta_p)$  for PAA with that of the CMC solution for the 2-mm capillary.

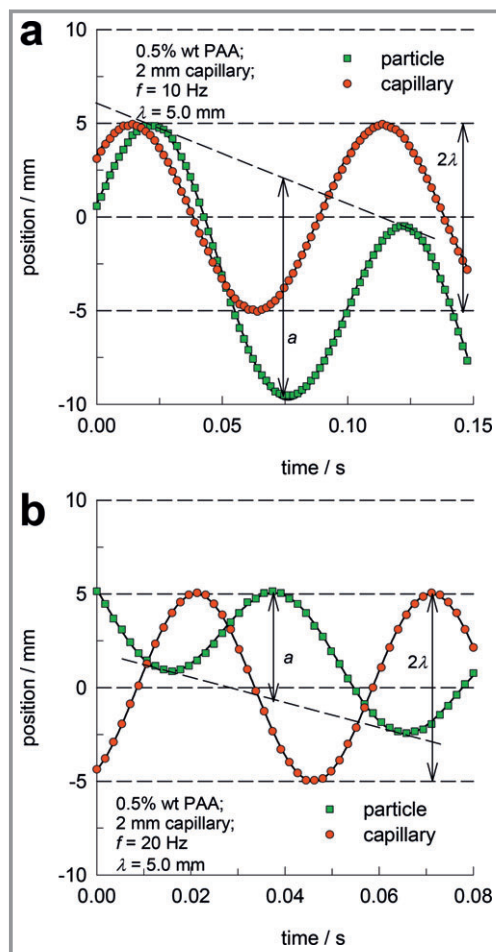


**Figure 9.** Typical examples of the high-speed movie analysis of the sinusoidal motion of the capillary tube and the tracer particle for 0.5 wt % PAA in a 2-mm capillary at vibration frequencies of a) 10 Hz and b) 20 Hz.

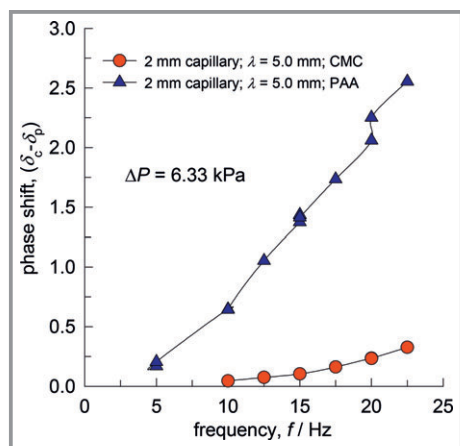


**Figure 10.** Comparison of the phase shift  $\delta_c - \delta_p$  for the flow of 0.5 wt % PAA in a 2-mm capillary with that of 0.7 wt % CMC solution.

Figs. 11a–c show the flow enhancement factor of a 0.5 wt % PAA solution as function of the vibration frequency in capillaries of 1, 2, and 4 mm diameter, respectively.

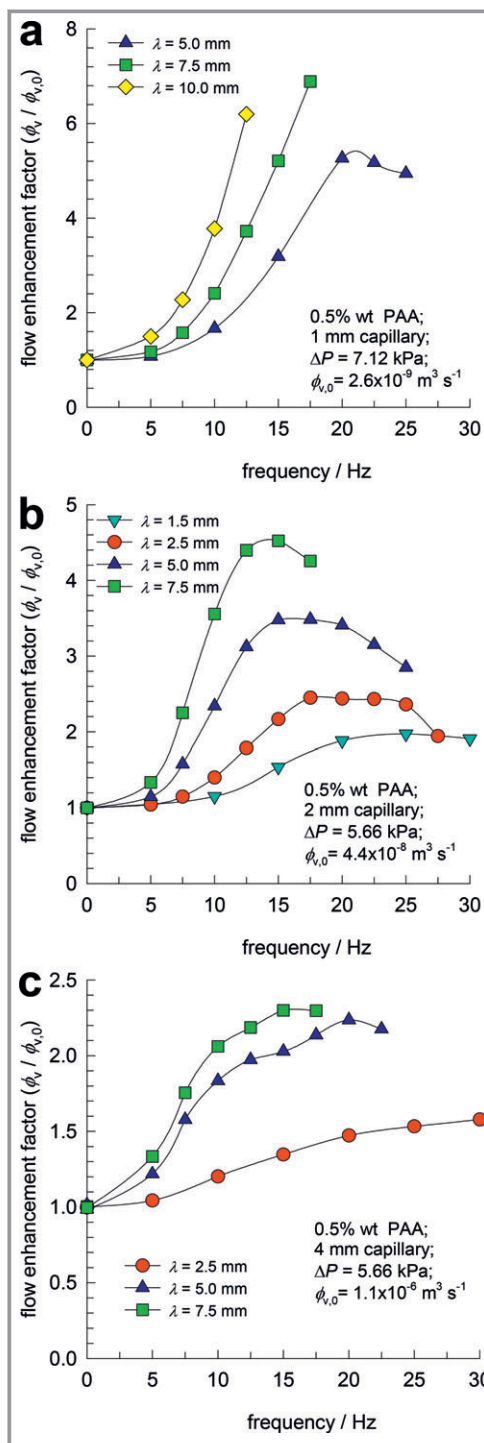


**Figure 11.** Flow enhancement factor of a 0.5 wt % PAA solution as function of the vibration frequency in capillaries of a) 1 mm, b) 2 mm, and c) 4 mm diameter.

Generally speaking, due to its lower apparent viscosity, the flow enhancement factor for PAA is lower than for CMC. Furthermore, the flow enhancement exhibits a pronounced maximum as the frequency is increased. The rea-

son for this is the increased phase shift, caused perhaps by the viscoelastic nature of PAA.

## 6 Conclusions

The application of sinusoidal vibrations in the longitudinal direction to the flow of shear-thinning CMC and PAA solutions inside capillary tubes results in a significant enhancement in the flow due to a decrease in the apparent viscosity. The flow enhancement factor depends on both the vibration frequency and the vibration amplitude; it is not a unique function of the vibration intensity  $\Gamma$ . Increasing the vibration amplitude or the vibration frequency, while keeping all the other operating conditions constant, always increases the flow enhancement factor. For PAA, the enhancement factor exhibits a maximum plateau value caused by the increase in the phase shift between the sinusoidal motion of the capillary wall and of the liquid within the tube. Increasing the pressure gradient in the tube decreases the flow enhancement factor.

This article has been submitted as felicitation of Prof. Dr. Frerich J. Keil on his 70th birthday. The authors would like to express their gratitude to Prof. Keil for introducing them to the influence of vibrations on hydrodynamics.

### Symbols used

$a$	[m]	amplitude of tracer particle
$b$	[m]	vertical shift parameter
$D$	[m]	inner diameter of capillary
$d_p$	[m]	particle diameter
$f$	[Hz]	vibration frequency
$g$	[m s <sup>-2</sup> ]	gravitational acceleration
$h$	[m]	position of the particle
$k$	[Pa s <sup>n</sup> ]	flow consistency index
$L$	[m]	length of the capillary
$n$	[-]	flow behavior index
$\Delta P$	[Pa]	pressure drop
$t$	[s]	time
$u$	[m s <sup>-1</sup> ]	particle velocity
$\langle u \rangle$	[m s <sup>-1</sup> ]	mean liquid velocity

### Greek symbols

$\dot{\gamma}$	[s <sup>-1</sup> ]	shear rate
$\Gamma$	[-]	vibration intensity, $\lambda(2\pi f)^2/g$
$\delta$	[-]	phase shift of particle in relation to the tube, $\delta_c - \delta_p$

$\delta_c$	[-]	phase shift of the capillary
$\delta_p$	[-]	phase shift of the particle
$\phi_m$	[kg s <sup>-1</sup> ]	mass flow rate
$\phi_v$	[m <sup>3</sup> s <sup>-1</sup> ]	volume flow rate
$\phi_{v,0}$	[m <sup>3</sup> s <sup>-1</sup> ]	steady-state volume flow rate
$\eta$	[Pa s]	dynamic viscosity
$\eta_a$	[Pa s]	apparent viscosity
$\lambda$	[m]	vibration amplitude
$\rho$	[kg m <sup>-3</sup> ]	liquid density
$\tau$	[Pa]	shear stress

### Abbreviations

CMC carboxymethylcellulose

PAA polyacrylamide

### References

- [1] H. A. Barnes, P. Townsend, K. Walters, *Rheol. Acta* **1971**, *10*, 517 – 527.
- [2] P. Townsend, *Rheol. Acta* **1973**, *12*, 13 – 18.
- [3] D. W. Sundstrom, A. Kaufman, *Ind. Eng. Chem. Process Des. Dev.* **1977**, *16*, 320 – 325.
- [4] B. Mena, O. Manero, D. M. Binding, *J. Non-Newtonian Fluid Mech.* **1979**, *5*, 427 – 448.
- [5] A. K. Deysarkar, G. A. Turner, *J. Rheol.* **1981**, *25*, 41 – 54.
- [6] N. Phan-Thien, J. Dudek, *J. Non-Newtonian Fluid Mech.* **1982**, *11*, 147 – 161.
- [7] J. A. Goshawk, N. D. Waters, *J. Non-Newtonian Fluid Mech.* **1994**, *54*, 449 – 464.
- [8] J. A. Goshawk, N. D. Waters, G. K. Rennie, E. J. Staples, *J. Non-Newtonian Fluid Mech.* **1994**, *51*, 21 – 60.
- [9] Y. Li, K. Shen, *J. Macromol. Sci., Part B: Phys.* **1994**, *46*, 785 – 792.
- [10] J. P. Ibar, *Polym. Eng. Sci.* **1998**, *38*, 1 – 20.
- [11] O. Manero, B. Mena, *Rheol. Acta* **2001**, *16*, 573 – 576.
- [12] J. H. He, Y. Q. Wan, J. Y. Yu, *Int. J. Nonlinear Sci. Numer. Simul.* **2004**, *5*, 253 – 262.
- [13] S. Shin, J. H. Lee, *Int. Commun. Heat Mass Transfer* **2002**, *29*, 1069 – 1077.
- [14] S. Shin, J. H. Lee, *Jpn. J. Appl. Phys.* **2003**, *42*, 1363 – 1367.
- [15] S. Shin, Y. Ku, M. S. Park, S. Y. Moon, J. S. Suh, *Clin. Hemorheol. Microcirc.* **2004**, *30*, 353 – 358.
- [16] A. N. Vavreck, *Int. J. Food Sci. Technol.* **2004**, *39*, 465 – 468.
- [17] G. S. Zeng, J. P. Qu, *J. Appl. Polym. Sci.* **2007**, *106*, 1152 – 1159.
- [18] N. S. Deshpande, M. Barigou, *Chem. Eng. Sci.* **2001**, *56*, 3845 – 3853.
- [19] M. Easa, M. Barigou, *Comput. Fluids* **2008**, *37*, 24 – 34.
- [20] R. Krishna, J. Ellenberger, M. I. Urseanu, F. J. Keil, *Naturwissenschaften* **2000**, *87*, 455 – 459.
- [21] J. Ellenberger, R. Krishna, *Enhancement of the Flow Rate of Shear-Thinning Liquids by Low Frequency Vibrations*, **2017**. <http://krishna.amsterchem.com/polymervibration/> (Accessed on April 24, 2017)
- [22] R. G. Sousa, M. L. Riethmuller, A. M. F. R. Pinto, J. B. L. M. Campos, *J. Non-Newtonian Fluid Mech.* **2006**, *135*, 16 – 31.